ARTICLE OPEN

Check for updates

Associations of plasma biomarkers with cerebral perfusion and structure in Alzheimer's disease

Yong He[1,4], Xiaojiao Liu[1,2,4], Fang Liu[1], Ping Che[1], Yanxin Zhang[1], Ruxue Fan[1], Yuan Li[1], Wen Qin[3] and Nan Zhang[1]✉

Plasma biomarkers have great potential in the screening, diagnosis, and monitoring of Alzheimer's disease (AD). However, findings on their associations with cerebral perfusion and structural changes are inconclusive. We examined both cross-sectional and longitudinal associations between plasma biomarkers and cerebral blood flow (CBF), gray matter (GM) volume, and white matter (WM) integrity. Forty-eight AD patients whose diagnosis was supported by amyloid-β (Aβ) PET received measurement of plasma biomarkers with a single molecular array, including Aβ42, phosphorylated tau 181 (P-tau181), neurofilament light (NfL), total tau (T-tau), and glial fibrillary acidic protein (GFAP), and both baseline and one-year follow-up magnetic resonance imaging, including pseudo-continuous arterial spin labeling, T1-weighted imaging, and diffusion tensor imaging. Correlations were found between regional CBF and several plasma biomarkers, with Aβ42 showing the strongest correlation with CBF in the left inferior temporal gyrus ($r = 0.507$, $p = 0.001$). Plasma P-tau181 and GFAP levels were correlated with GM volume in the posterior cingulate gyrus and the bilateral hippocampus and right middle temporal gyrus, respectively. Decreased CBF and GM volume in regions vulnerable to AD, such as the posterior cingulate gyrus, inferior parietal lobule and hippocampus, could be predicted by the levels of specific plasma biomarkers. Most biomarkers, except Aβ42, showed extensive correlations with longitudinal WM disruption. Plasma biomarkers exhibited varied correlations with brain perfusion, GM volume, and WM integrity and predicted their longitudinal changes in AD patients, suggesting their potential to reflect functional and structural changes and to monitor pathophysiological progression in the brain.

Translational Psychiatry (2025)15:2 ; https://doi.org/10.1038/s41398-024-03220-3

INTRODUCTION

Currently, the diagnosis of Alzheimer's disease (AD) is based on clinical presentations and postmortem confirmation but can also be made in vivo with the presence of abnormal biomarkers [1]. Although cerebrospinal fluid (CSF) and positron emission tomography (PET) biomarkers have largely increased diagnostic accuracy, they are either invasive or expensive to identify. With the development of ultrasensitive immunoassays and mass spectrometry techniques, biomarkers can be identified in peripheral blood with great performance. Blood-based biomarkers are easily accessible, cost- and time-effective, less invasive, and can be serially measured, which suggests new possibilities in the screening, diagnosis, and monitoring of AD [2].

Recent studies have identified and validated plasma biomarkers reflecting pathological processes involved in the occurrence and progression of AD, including amyloid-β (Aβ) deposition (Aβ42 and Aβ42/40), pathological tau [phosphorylated tau (P-tau)], neurodegeneration [neurofilament light (NfL) and total tau (T-tau)], and neuroinflammation [glial fibrillary acidic protein (GFAP)], as the ATNI profile [3, 4]. Given the promising application of these plasma biomarkers in clinical practice and trials, it is important to clarify their correlations with various pathophysiological mechanisms, such as functional and structural changes in the brain, in addition to their diagnostic value in AD.

Several studies have cross-sectionally and longitudinally observed correlations between gray matter (GM) atrophy and the levels of plasma biomarkers, such as P-tau181, NfL, T-tau, and GFAP [5–8], although the results were not comparable or were inconsistent between different testing platforms. Apart from brain volume reduction, white matter (WM) disruption and decreased cerebral blood flow (CBF) have been found to be evident even at early stages of AD [9–13] and could be direct causes of cognitive impairment [14–17]. Plasma biomarkers, such as P-tau181, NfL, and GFAP, have been reported to be correlated with WM integrity in AD patients [18–20]. However, whether plasma biomarkers can reflect CBF changes in AD patients has not been investigated. Aβ and tau depositions can be accelerated by cerebral hypoperfusion, and in turn, the neurotoxic Aβ and tau further exacerbate cerebral hypoperfusion [21–24].

Therefore, although a few studies have reported associations between specific plasma biomarkers and GM and WM changes, a comprehensive understanding of how ATNI plasma biomarkers can reflect functional and structural brain changes, particularly perfusion, is lacking. In this study, we analyzed the plasma levels of Aβ42, P-tau181, NfL, T-tau, and GFAP and their correlations with

[1]Department of Neurology, Tianjin Neurological Institute, Tianjin Medical University General Hospital, Tianjin, China. [2]Department of Neurology, Tianjin Medical University General Hospital Airport Site, Tianjin, China. [3]Department of Radiology and Tianjin Key Laboratory of Functional Imaging, Tianjin Medical University General Hospital, Tianjin, China. [4]These authors contributed equally: Yong He, Xiaojiao Liu. ✉email: nkzhangnan@yeah.net

Received: 15 June 2024 Revised: 6 December 2024 Accepted: 27 December 2024
Published online: 06 January 2025

cross-sectional and longitudinal changes in CBF, GM volume, and WM integrity measured with magnetic resonance imaging (MRI) in AD patients whose diagnosis was supported by amyloid PET.

METHODS

Participants

A total of 72 participants (48 AD patients and 24 cognitively unimpaired controls) were recruited from Tianjin Medical University General Hospital. This was an exploratory study. Empirical and feasibility considerations determined the number of enrolled participants. No formal statistical estimation of sample size was performed. All participants provided written informed consent. The diagnosis of AD was based on the research criteria for typical AD of the International Working Group-2 (IWG-2) [25]. The inclusion criteria for AD patients were as follows: (1) aged 50–85 years; (2) had early and prominent episodic memory impairment; (3) had a Clinical Dementia Rating (CDR) [26] score of 0.5–2; (4) had a positive result on ^{11}C-Pittsburgh Compound B (PiB) PET; and (5) had no evidence of clinically significant cerebrovascular lesions on MRI. Patients whose cognitive impairment was potentially caused by other neurological diseases, mental disorders or medical conditions, such as frontotemporal lobar degeneration, Parkinson's disease dementia or dementia with Lewy bodies, multiple sclerosis, severe depression, alcohol or drug abuse, vitamin B12 deficiency, or human immunodeficiency virus (HIV) or syphilis infection, were excluded. The inclusion criteria for the cognitively unimpaired (CU) controls were as follows: (1) aged 50–85 years; (2) no subjective cognitive decline complaints and normal performance in each cognitive domain of objective neuropsychological tests; (3) a CDR score of 0 and a Mini-Mental State Examination (MMSE) [27] score no less than 24; and (4) no clinically significant brain atrophy or cerebrovascular lesions on MRI. Plasma biomarkers and both concurrent and one-year follow-up neuroimaging data were collected for all participants.

Measurement of plasma biomarkers

Blood samples were collected in EDTA tubes in the morning. The samples were centrifuged at 2500 × *g* and 4 °C for 35 min to obtain plasma within 2 h of collection. The plasma samples were stored at −80 °C for future analysis. Plasma biomarkers were measured using single molecular array technology with an ultrahigh-sensitivity protein molecular detection instrument (Simoa HD-1, Quanterix, MA, USA). Plasma Aβ42 and T-tau levels were measured using a Neurology 3-Plex A assay kit (Quanterix, 503203), NfL, and GFAP levels were measured using a Neurology 2-Plex B assay kit (Quanterix, 502713), and P-tau181 levels were measured using a P-tau181 V2 assay kit (Quanterix 503008) according to the manufacturer's instructions.

MRI acquisition

MRI was performed on a 3.0-Tesla scanner (Discovery MR750, General Electric, Milwaukee, WI) with a 64-channel phased array head coil. T1 images were obtained using a brain volume (BRAVO) sequence with the following parameters: echo time (TE)/repetition time (TR) = 3.18/8.16 ms, inversion time (TI) = 450 ms, field of view (FOV) = 256 × 256 mm, matrix = 256 × 256, flip angle (FA) = 12°, slice thickness = 1 mm, and 188 slices. The 3D pseudo-continuous arterial spin labeling (ASL) series was acquired using a spiral spin–echo sequence and background suppression with the following parameters: TE/TR = 11.1/5046 ms, labeling duration = 1450 ms, post-labeling delay (PLD) = 2025 ms, FA = 111°, matrix size = 128 × 128, FOV = 240 × 240 mm, arms = 8, acquisition points = 512, slice thickness = 3 mm, and 50 slices. Diffusion MRI was acquired using a diffusion-weighted spin–echo single shot echo planar imaging (EPI) sequence with the following parameters: TE/TR = 63.2/6000 ms, FA = 90°, FOV = 256 × 256 mm, matrix size = 128 × 128, slice thickness = 6 mm, 50 slices, and 64 diffusion directions (b = 1000 s/mm^2).

Image processing

ASL MRI images were automatically converted into CBF maps using Functool software (version 9.4, GE Medical Systems) on an Advantage Windows workstation. Image processing was conducted using voxel-based analysis in SPM12 (https://www.fil.ion.ucl.ac.uk/spm/software/spm12) with the following steps: (1) the CBF images were registered to structural MRI images; (2) the structural images were normalized to the Montreal Neurological Institute (MNI) space and segmented into GM, WM and CSF; (3) using the parameters determined from the structural images, the CBF images were normalized and multiplied by a binary brain tissue mask consisting of only GM and WM; and (4) the normalized CBF maps were then smoothed with a full width at half maximum (FWHM) of 10 mm. We performed a quality check via visual inspection at every preprocessing stage. The differences in CBF between AD patients and CU controls were analyzed using two-sample t tests with age and sex as covariates. Several clusters were identified after adjusting for global values with an analysis of covariance (ANCOVA) (voxelwise threshold $p < 0.001$, minimum cluster size 100 voxels). Significant regions were identified with Talairach–Daemon software (Research Imaging Center, University of Texas Health Science Center, San Antonio, TX, USA). To quantify the CBF changes in specific cortical regions, we further used a 4-mm radius spherical volume of interest (VOI) centered at the peak voxel of those clusters that were significant in the SPM analyses. Finally, we obtained the relative CBF values by calculating the ratios of the regional CBF values to the global CBF values in all participants. We used the relative CBF values for cross-sectional analysis and changes in absolute regional CBF values for longitudinal analysis.

T1 images were processed using voxel-based morphometry (VBM) analysis in SPM12 with the CAT12 toolbox (http://www.neuro.uni-jena.de/cat) as previously described [28]. Briefly, images were preprocessed by denoising, bias correction and intensity normalization. Then, the preprocessed images were normalized to the MNI space using affine and nonlinear registration and segmented into GM, WM, and CSF. Furthermore, to preserve the total amount of GM in the original image, segmented GM images were modulated by scaling with the amount of GM change caused by image registration. Finally, the resultant GM images were smoothed with an FWHM of 8 mm. The total intracranial volume (TIV) was calculated as the sum of the total volume of GM, WM and CSF estimated during the VBM analysis using CAT12. A quality check via visual inspection was conducted at every preprocessing stage. Two-sample t-tests were used to identify group differences in GM volume between AD patients and CU controls using the CAT12 statistical module with age, sex, and TIV as covariates. According to the default settings for CAT12, we used 0.1 as the absolute masking threshold for the VBM data. With a voxel-level peak threshold of $p < 0.001$ (uncorrected), we primarily identified clusters >100 voxels for the analysis. Significant regions were identified with Talairach–Daemon software. To quantify the GM volume in specific regions, we further used a 4-mm radius of spherical VOI centered at the peak voxel of those clusters that were significant in the SPM analyses. Finally, we acquired the GM volume for each VOI, which was adjusted for TIV.

DTI data were processed using the FMRIB's Diffusion Toolbox (FDT) in the FMRIB Software Library (FSL V.6.0) (https://fsl.fmrib.ox.ac.uk/fsl/fsl). Images were preprocessed with the following steps: (1) eddy-current correction for EPI distortion correction; (2) skull removal and brain tissue extraction using a brain extraction toolbox; and (3) extraction of average fractional anisotropy (FA) values within the fiber tracts. To compare WM integrity between AD patients and CU controls, voxelwise analysis of FA data was carried out using tract-based spatial statistics (TBSS) [29] with the following steps: (1) the individual FA maps were nonlinearly registered to the MNI space using a default FMRIB58_FA atlas; (2) the normalized FA maps were averaged to generate a mean FA image and then skeletonized to generate a mean FA skeleton map with a threshold of 0.2; (3) an individual FA skeleton map was obtained by projecting the normalized individual FA map onto the mean FA skeleton map; and (4) a general linear model was generated with a nonparametric permutation-based inference ("randomize" program within FSL) with age and sex as covariates. The number of permutations was set to 5000. A familywise error method ($p < 0.05$) was used to correct for multiple comparisons using the threshold-free cluster enhancement (TFCE) option in the permutation testing tool in FSL. We selected significant WM fibers and labeled them according to the ICBM-DTI-81 WM label atlas [30]. Finally, we extracted the FA values of these WM fibers in MATLAB (version R2016a, MathWorks, Natick, MA, United States).

Statistical analysis

Statistical analyses were performed using SPSS 26.0. A two-tailed $p < 0.05$ was considered to indicate statistical significance. Demographic and clinical data were compared between AD patients and CU controls using Student's t-tests for continuous variables and chi-square tests for dichotomous variables. Partial correlation analysis adjusted for age and sex was conducted to examine the cross-sectional and longitudinal associations between each plasma biomarker and each neuroimaging measure in AD patients. Longitudinal changes in absolute regional CBF,

Table 1. Demographic, clinical, and plasma biomarker data of AD patients and CU controls.

	AD (N = 48)	CU (N = 24)	χ^2/t	p
Age, years	67.88 (7.47)	65.63 (6.27)	1.268	0.209
Sex, males	15 (31.25%)	13 (54.17%)	3.536	0.060
Education, years	10.54 (3.30)	11.92 (3.28)	−1.672	0.099
MMSE score	18.58 (5.12)	27.63 (1.47)	−11.339	**<0.001**
Plasma $A\beta_{42}$, pg/ml	14.04 (4.76)	17.15 (4.52)	−2.654	**0.010**
Plasma P-tau181, pg/ml	6.75 (1.95)	3.05 (1.02)	10.571	**<0.001**
Plasma NfL, pg/ml	1.24 (0.21)	0.95 (0.24)	5.230	**<0.001**
Plasma T-tau, pg/ml	2.29 (1.04)	2.39 (0.79)	1.847	0.070
Plasma GFAP, pg/ml	2.32 (0.20)	1.89 (0.22)	8.249	**<0.001**

Data are presented as the mean (SD) for continuous data and n (%) for dichotomous data. The plasma NfL and GFAP levels were log-transformed to normalize the distributions.
AD Alzheimer's disease, *CU* cognitively unimpaired, *MMSE* mini-mental state examination, *Aβ* amyloid-β, *P-tau* phosphorylated tau, *GFAP* glial fibrillary acidic protein, *NfL* neurofilament light, *T-tau* total tau.
Bold values identify statistical significance ($p < 0.05$).

GM volume, and FA values for each AD patient were calculated by subtracting the baseline value from the follow-up value for brain regions with significant differences from group comparisons. For neuroimaging measures, we focused on brain regions with significant differences between AD patients and CU controls. Continuous variables were tested for normal distribution and homoscedasticity using Shapiro–Wilk and Levene's tests. The plasma NfL and GFAP levels were log-transformed for partial correlation analysis to normalize their distributions.

RESULTS

Demographic and clinical characteristics and plasma biomarkers of all participants

Table 1 shows the baseline characteristics of all participants. There were no significant differences in age, sex, or years of education between the groups. MMSE scores were much lower in AD patients than in CU controls. Compared with CU controls, AD patients had lower plasma Aβ42 levels and higher plasma P-tau181, NfL, and GFAP levels ($p < 0.001$). The plasma T-tau level did not significantly differ between the groups.

Differences in CBF, GM volume, and WM integrity between AD patients and CU controls

Compared with that in CU controls, regional CBF in AD patients was relatively lower in the bilateral superior parietal lobule, bilateral inferior parietal lobule, bilateral posterior cingulate gyrus, bilateral uncus, left inferior temporal gyrus, right fusiform gyrus and left middle frontal gyrus and relatively greater in the right postcentral gyrus, right precentral gyrus, bilateral putamen, bilateral thalamus, left middle cingulate gyrus, and cerebellum after ANCOVA normalization for global CBF (Fig. 1).

The brain regions with decreased GM volume in the AD patients included the bilateral hippocampus, bilateral middle temporal gyrus, bilateral inferior parietal lobule, posterior cingulate gyrus, left superior frontal gyrus, left middle frontal gyrus, and left middle occipital gyrus (Fig. 2).

FA values were lower in the corpus callosum, bilateral coronal radiation, right sagittal stratum, bilateral cingulum and right superior longitudinal fasciculus of AD patients than in those of CU controls (Fig. 3).

Cross-sectional associations between plasma biomarkers and neuroimaging measures

Some associations between plasma biomarkers and neuroimaging measures were observed (Table 2), although they were no longer statistically significant after Bonferroni correction for multiple comparisons.

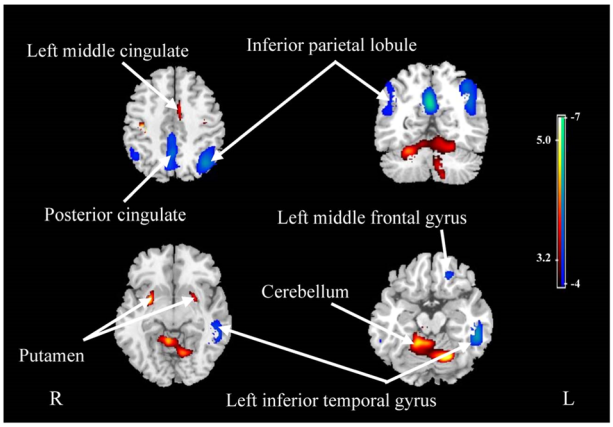

Fig. 1 Regions with relative CBF changes in AD patients compared with those in CU controls after ANCOVA for global CBF values. Cold colors indicate regions with relatively reduced CBF, and warm colors indicate regions with relatively increased CBF. The color bar represents t values for significant voxels. A threshold of 3.23 ($p < 0.001$, uncorrected) was used to overlay SPM maps onto a standard MRI brain template.

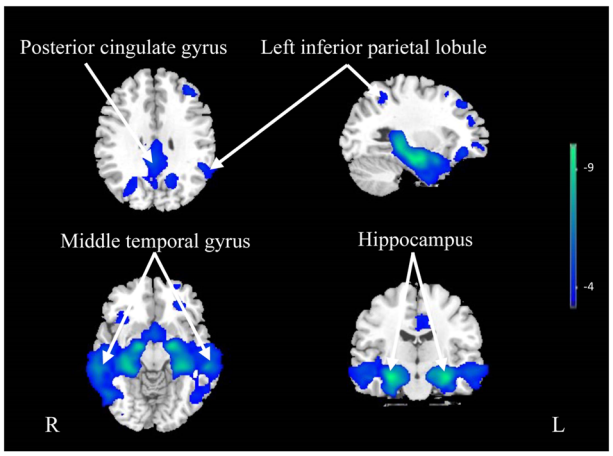

Fig. 2 Regions with GM atrophy in AD patients compared with CU controls. The color bar represents t values for significant voxels. A threshold of 3.23 ($p < 0.001$, uncorrected) was used to overlay SPM maps onto a standard MRI brain template.

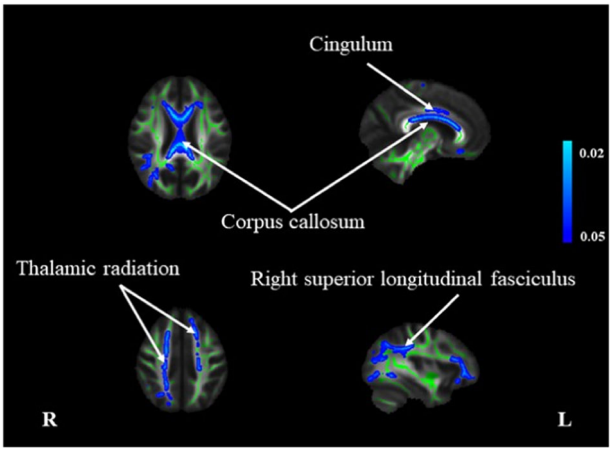

Fig. 3 Regions with reduced FA in AD patients compared with CU controls. All regions are overlaid on the mean FA template in grayscale and the associated FA template skeleton (shown in green). Blue represents areas of significantly reduced FA in AD patients ($p < 0.05$, FWE corrected).

Table 2. Cross-sectional correlations between plasma biomarkers and neuroimaging measures in AD patients.

	r	*p*
CBF		
Plasma Aβ42		
Left inferior temporal gyrus	0.507	0.001
Left inferior parietal lobule	0.460	0.003
Left superior parietal lobule	0.349	0.029
Right fusiform gyrus	0.321	0.047
Right postcentral gyrus	−0.411	0.009
Plasma NfL		
Left inferior parietal lobule	−0.363	0.025
Left superior parietal lobule	−0.336	0.039
Right precentral gyrus	0.461	0.004
Plasma T-tau		
Left cerebellum	0.346	0.031
Plasma GFAP		
Left inferior temporal gyrus	−0.332	0.039
Left middle cingulate gyrus	0.419	0.008
Right postcentral gyrus	0.345	0.031
Right putamen	0.359	0.025
GM volume		
Plasma P-tau181		
Posterior cingulate gyrus	−0.324	0.028
Plasma GFAP		
Left hippocampus	−0.429	0.003
Right hippocampus	−0.423	0.003
Right middle temporal gyrus	−0.322	0.029

The plasma NfL and GFAP levels were log-transformed. The partial correlation coefficients (r) were adjusted for age and sex. *CBF* cerebral blood flow, *Aβ* amyloid-β, *P-tau* phosphorylated tau, *GM* gray matter, *NfL* neurofilament light, *T-tau* total tau, *GFAP* glial fibrillary acidic protein.

Specifically, extensive correlations between plasma biomarkers and regional CBF were observed. Across all plasma biomarkers, Aβ42 demonstrated the strongest correlation with regional CBF in the left inferior temporal gyrus ($r = 0.507$, $p = 0.001$). Plasma Aβ42 levels were also correlated with regional CBF in the left inferior parietal lobule ($r = 0.460$, $p = 0.003$), left superior parietal lobule ($r = 0.349$, $p = 0.029$), right fusiform gyrus ($r = 0.321$, $p = 0.047$), and right postcentral gyrus ($r = -0.411$, $p = 0.009$). In addition, plasma NfL levels were correlated with regional CBF in the left inferior parietal lobule ($r = -0.363$, $p = 0.025$), left superior parietal lobule ($r = -0.336$, $p = 0.039$), and right precentral gyrus ($r = 0.461$, $p = 0.004$); plasma T-tau levels were correlated with regional CBF in the left cerebellum ($r = 0.346$, $p = 0.031$); and plasma GFAP levels were correlated with regional CBF in the left inferior temporal gyrus ($r = -0.332$, $p = 0.039$), left middle cingulate gyrus ($r = 0.419$, $p = 0.008$), right putamen ($r = 0.359$, $p = 0.025$), and right postcentral gyrus ($r = 0.345$, $p = 0.031$).

For GM volume, both plasma P-tau181 and GFAP levels showed correlations with several brain regions. The plasma GFAP level was correlated with the GM volume in the left hippocampus ($r = -0.429$, $p = 0.003$), right hippocampus ($r = -0.423$, $p = 0.003$), and right middle temporal gyrus ($r = -0.322$, $p = 0.029$); the plasma P-tau181 level was correlated with the GM volume in the posterior cingulate gyrus ($r = -0.342$, $p = 0.028$).

No associations were found between any plasma biomarker levels and FA values of WM fibers.

Associations between plasma biomarkers and longitudinal changes in neuroimaging findings

AD patients completed follow-up evaluations of CBF, GM volume, and WM integrity, with a median follow-up of 13 months (interquartile range = 3.5 months). Longitudinal changes in all neuroimaging indicators were calculated by subtracting the baseline values from the follow-up values. Some associations were observed between plasma biomarkers and longitudinal changes in neuroimaging measures (Table 3), although they were no longer statistically significant after Bonferroni correction for multiple comparisons. Specifically, plasma Aβ42 and P-tau181 levels were correlated with longitudinal CBF changes in the right posterior cingulate gyrus ($r = 0.388$, $p = 0.041$) and right inferior parietal lobule ($r = -0.385$, $p = 0.043$), respectively.

Plasma Aβ42 ($r = 0.463$, $p = 0.006$) and GFAP ($r = -0.457$, $p = 0.007$) levels were significantly correlated with changes in GM volume in the left inferior parietal lobule. In addition, the plasma T-tau level was correlated with changes in GM volume in the right hippocampus ($r = -0.384$, $p = 0.025$).

Plasma P-tau181, NfL, T-tau, and GFAP levels predicted FA decline in several WM fiber tracts; specifically, P-tau181 levels predicted FA decline in WM fiber tracts in the splenium of the corpus callosum, bilateral cingulum, right hippocampal cingulum, right superior longitudinal fasciculus and bilateral coronal radiation; GFAP levels predicted FA decline in WM fiber tracts in the genu of the corpus callosum, body of the corpus callosum, right cingulum and left posterior coronal radiation; and NfL levels predicted FA decline in WM fiber tracts in the body of the corpus callosum, left cingulum and right posterior coronal radiation; and T-tau for left superior coronal radiation.

DISCUSSION

The present study examined both cross-sectional and longitudinal associations between plasma biomarkers and neuroimaging measures in AD patients. We found that plasma biomarkers

Table 3. Associations between plasma biomarkers and longitudinal changes in neuroimaging measures.

	r	p
CBF		
Plasma Aβ42		
Right posterior cingulate gyrus	0.388	0.041
Plasma P-tau181		
Right inferior parietal lobule	−0.385	0.043
GM volume		
Plasma Aβ42		
Left inferior parietal lobule	0.463	0.006
Plasma T-tau		
Right hippocampus	−0.384	0.025
Plasma GFAP		
Left inferior parietal lobule	−0.457	0.007
FA		
Plasma P-tau181		
Splenium of corpus callosum	−0.378	0.027
Left cingulum	−0.392	0.022
Right cingulum	−0.356	0.039
Right hippocampal cingulum	−0.427	0.012
Right superior longitudinal fasciculus	−0.364	0.035
Right superior coronal radiation	−0.421	0.013
Right posterior coronal radiation	−0.341	0.048
Plasma NfL		
Body of corpus callosum	−0.394	0.021
Left cingulum	−0.359	0.037
Right posterior coronal radiation	−0.480	0.004
Plasma T-tau		
Left superior coronal radiation	−0.377	0.031
Plasma GFAP		
Genu of corpus callosum	−0.403	0.018
Body of corpus callosum	−0.412	0.016
Right cingulum	−0.343	0.047
Left posterior coronal radiation	−0.405	0.017

The plasma NfL and GFAP levels were log-transformed. The partial correlation coefficients (r) were adjusted for age and sex. *CBF* cerebral blood flow, *Aβ* amyloid-β, *GM* gray matter, *FA* fractional anisotropy, *P-tau* phosphorylated tau, *NfL* neurofilament light, *T-tau* total tau, *GFAP* glial fibrillary acidic protein.

correlated differently with brain perfusion, GM volume, and WM integrity and predicted their changes in patients with AD. In general, plasma biomarkers showed extensive correlations with regional CBF, in particular the amyloid biomarker (Aβ42); the amyloid biomarker (Aβ42) and tau biomarker (P-tau181) were also predictive of CBF decline. The neuroinflammation biomarker (GFAP) was the main biomarker correlated with regional brain volume and longitudinal loss of brain volume. Although there was no association between any biomarker and FA values at baseline, all biomarkers except Aβ42 showed correlations with regional WM deterioration at follow-up.

Aβ, the main pathological hallmark of AD, is believed to initiate and facilitate a series of pathophysiological processes in the pathogenesis of AD [31, 32]. We found that a lower plasma Aβ42 level predicted greater atrophy in the left inferior parietal lobule in AD patients. A previous study reported that lower plasma Aβ42/40 ratios were associated with atrophy in the occipital and temporal cortices in a Chinese cohort including participants with normal cognition, mild cognitive impairment (MCI), AD, and non-AD dementia [33]. These findings were also supported by PET studies that showed a relationship between high amyloid deposition and GM atrophy, particularly in the temporal and parietal regions in cognitively impaired patients [34].

Although correlations between plasma amyloid biomarkers and cerebral perfusion have not been reported, plasma Aβ42 levels are strongly correlated with regional CBF changes, particularly in the temporoparietal region, in AD patients. This finding was supported by a previous study in which brain Aβ load measured by PET was associated with decreased CBF in temporoparietal regions in patients with MCI and AD [35]. Furthermore, a correlation between Aβ pathology and cerebral hypoperfusion was demonstrated in transgenic AD mice [36]. In turn, increased Aβ accumulation in the brain was observed in mouse models of chronic cerebral hypoperfusion [24, 37].

Plasma P-tau181, which has been demonstrated to be a specific AD biomarker, was significantly increased in AD patients compared with that in CU individuals and was highly correlated with CSF P-tau181 and tau PET [38]. Associations between plasma P-tau181 and brain atrophy in AD-vulnerable regions have been established cross-sectionally and longitudinally in cognitively impaired individuals [39, 40]. In our study, we observed that plasma P-tau181 was associated with posterior cingulate atrophy but did not predict GM atrophy over time. An association between plasma P-tau181 and longitudinal GM volume loss in AD dementia patients was not observed in previous studies [5, 39].

Very few studies have explored the association between plasma P-tau181 and cerebral perfusion changes and WM microstructural damage. Although we did not find cross-sectional associations of plasma P-tau181 with either regional CBF or FA, baseline levels of plasma P-tau181 could predict CBF reduction in the right inferior parietal lobule and FA decline in several brain areas, such as the splenium of the corpus callosum, bilateral coronal radiation, cingulum, and right superior longitudinal fasciculus. Similarly, it has been found that plasma P-tau181 was associated with longitudinal hypometabolism measured by fluorine-18–labeled fluorodeoxyglucose (FDG) PET in typical AD regions [41]. For WM integrity, one study reported cross-sectional associations between plasma P-tau181 and reduced FA in the left hippocampal cingulum, left fornix, and left medial lemniscus in AD patients [18]. These findings suggested the potential effect of P-tau pathology on brain perfusion and WM integrity.

Plasma GFAP is a marker of astrogliosis. Despite not being specific to AD, plasma GFAP levels were found to be significantly elevated in individuals within the AD continuum compared with that in CU individuals [8, 42, 43]. Our study revealed extensive associations between plasma GFAP levels and all neuroimaging measures, including CBF, GM volume, and WM integrity. Specifically, plasma GFAP was significantly correlated with GM atrophy in the bilateral hippocampus and right middle temporal gyrus, predicted GM loss in the left inferior parietal lobule, was negatively correlated with decreased CBF in the left inferior temporal gyrus, and predicted FA decline in several WM tracts, including the genu of the corpus callosum, body of the corpus callosum, left coronal radiation and right cingulum. This is not surprising due to the involvement of reactive astrocytes in various pathophysiological processes in neurodegenerative diseases, e.g., AD [44–46]. It was previously observed that an increased plasma GFAP level was related to brain atrophy [33, 47], hypometabolism [8], and WM disruption [20] in regions vulnerable to AD.

NfL and T-tau are markers of axonal injury that are not specific to a particular disease but are linked to neurodegeneration processes. Previous studies reported associations between plasma NfL levels and brain atrophy in the temporal, parietal and frontal regions in AD patients [6, 48, 49]. However, we did not observe correlations between plasma NfL levels and GM volume, which is consistent with the

findings of other studies [33, 50]. AD patients have been shown to have different patterns of brain atrophy, such as medial-temporal predominant atrophy, parieto-occipital atrophy, mild atrophy, and diffuse cortical atrophy [51], which may explain the negative results for the correlations of specific brain regions. Moreover, clinical and pathological stages of AD patients could vary across different studies. Brain atrophy is usually subtle in the early stages but plateaus in very late stages. Finally, since a larger sample size is more likely to produce a positive result according to previous studies, the correlation between plasma NfL level and brain atrophy needs to be further investigated in a large cohort including AD patients at various stages. In our study, the plasma NfL level was correlated with changes in the CBF in the left inferior parietal lobule and right precentral gyrus and could predict FA decline in the body of the corpus callosum, left cingulum and right posterior coronal radiation. The perfusion correlation was supported by previous findings that plasma NfL was negatively associated with the FDG composite score of AD-typical hypometabolic regions, such as the bilateral angular, temporal, and posterior cingulate [6]. Previous studies also revealed a correlation between plasma NfL levels and WM degeneration in MCI patients [19]. Moreover, plasma T-tau levels predicted GM loss in the right hippocampus and FA decline in the left superior coronal radiation in our study. These findings were consistent with a previous study in which plasma T-tau predicted hippocampal atrophy over time, whereas no baseline association was found [7]. Moreover, other studies revealed cross-sectional associations between the plasma T-tau level and lower cortical thickness in the temporal, parietal, and frontal regions [52, 53].

Our study has several strengths. First, we incorporated a relatively full picture of plasma biomarkers in the same cohort and used the same detection methods, making the results consistent and comparable. In addition, we explored various aspects of brain changes involved in AD pathogenesis using MRI, particularly cerebral perfusion, which has rarely been investigated for its correlation with AD biomarkers. Finally, we obtained longitudinal MRI data, allowing us to test the ability of plasma biomarkers to predict brain structural and functional changes over time. However, some limitations of the current study should be noted. First, the relatively small number of participants reduced the representativeness of the whole AD population and may have led to some false-negative results. In addition, all the correlations observed in our study were no longer statistically significant after multiple comparison correction, which means there may be some false-positive results. As an exploratory study, the results show the tendency of changes to provide more possibilities for subsequent validation in larger cohorts. Second, the patients were followed for only ~1 year. A previous study revealed that rates of AD-specific cortical thinning increased with disease progression during the early stages of AD and started to decline when the MMSE score was approximately less than 21 [54]. Thus, the short follow-up period may decrease the possibility of identifying biomarkers of disease and pathophysiological progression. Moreover, we did not perform longitudinal measurements of plasma biomarkers, potentially preventing us from identifying more noticeable effects. Finally, single-PLD ASL was used in this study. Although single-PLD may result in the inaccurate estimation of CBF and is unable to capture the dynamic nature of CBF, compared with multiple-PLD, this method has a simple acquisition process, shorter scanning time, and easier data processing.

In conclusion, our findings suggest that plasma biomarkers not only are useful for the clinical diagnosis and differentiation of AD but also provide additional information on functional and structural brain changes, particularly for predicting decreases in cerebral perfusion, GM volume, and WM integrity.

DATA AVAILABILITY

The datasets generated and analyzed during the current study are available from the corresponding author on reasonable request.

REFERENCES

1. Jack CR, Bennett DA, Blennow K, Carrillo MC, Dunn B, Haeberlein SB, et al. NIA-AA research framework: toward a biological definition of Alzheimer's disease. Alzheimers Dement. 2018;14:535–62.
2. O'Bryant SE, Mielke MM, Rissman RA, Lista S, Vanderstichele H, Zetterberg H, et al. Blood-based biomarkers in Alzheimer disease: current state of the science and a novel collaborative paradigm for advancing from discovery to clinic. Alzheimers Dement. 2017;13:45–58.
3. Teunissen CE, Verberk IMW, Thijssen EH, Vermunt L, Hansson O, Zetterberg H, et al. Blood-based biomarkers for Alzheimer's disease: towards clinical implementation. Lancet Neurol. 2022;21:66–77.
4. Imbimbo BP, Watling M, Imbimbo C, Nisticò R. Plasma ATN(I) classification and precision pharmacology in Alzheimer's disease. Alzheimers Dement. 2023;19:4729–34.
5. Karikari TK, Pascoal TA, Ashton NJ, Janelidze S, Benedet AL, Rodriguez JL, et al. Blood phosphorylated tau 181 as a biomarker for Alzheimer's disease: a diagnostic performance and prediction modelling study using data from four prospective cohorts. Lancet Neurol. 2020;19:422–33.
6. Mattsson N, Cullen NC, Andreasson U, Zetterberg H, Blennow K. Association between longitudinal plasma neurofilament light and neurodegeneration in patients with Alzheimer disease. JAMA Neurol. 2019;76:791–9.
7. Mattsson N, Zetterberg H, Janelidze S, Insel PS, Andreasson U, Stomrud E, et al. Plasma tau in Alzheimer disease. Neurology. 2016;87:1827–35.
8. Shen X-N, Huang S-Y, Cui M, Zhao Q-H, Guo Y, Huang Y-Y, et al. Plasma glial fibrillary acidic protein in the Alzheimer disease continuum: relationship to other biomarkers, differential diagnosis, and prediction of clinical progression. Clin Chem. 2023;69:411–21.
9. Chen Y, Wang Y, Song Z, Fan Y, Gao T, Tang X. Abnormal white matter changes in Alzheimer's disease based on diffusion tensor imaging: a systematic review. Ageing Res Rev. 2023;87:17.
10. Brueggen K, Dyrba M, Cardenas-Blanco A, Schneider A, Fliessbach K, Buerger K, et al. Structural integrity in subjective cognitive decline, mild cognitive impairment and Alzheimer's disease based on multicenter diffusion tensor imaging. J Neurol. 2019;266:2465–74.
11. Korte N, Nortley R, Attwell D. Cerebral blood flow decrease as an early pathological mechanism in Alzheimer's disease. Acta Neuropathol. 2020;140:793–810.
12. Zhang H, Wang Y, Lyu D, Li Y, Li W, Wang Q, et al. Cerebral blood flow in mild cognitive impairment and Alzheimer's disease: a systematic review and meta-analysis. Ageing Res Rev. 2021;71:9.
13. Wierenga CE, Hays CC, Zlatar ZZ. Cerebral blood flow measured by arterial spin labeling MRI as a preclinical marker of Alzheimer's disease. J Alzheimers Dis. 2014;42:S411–9.
14. O'Donovan J, Watson R, Colloby SJ, Blamire AM, O'Brien JT. Assessment of regional MR diffusion changes in dementia with Lewy bodies and Alzheimer's disease. Int Psychogeriatr. 2014;26:627–35.
15. Wang Y, West JD, Flashman LA, Wishart HA, Santulli RB, Rabin LA, et al. Selective changes in white matter integrity in MCI and older adults with cognitive complaints. Biochim Biophys Acta Mol Basis Dis. 2012;1822:423–30.
16. Leeuwis AE, Benedictus MR, Kuijer JPA, Binnewijzend MAA, Hooghiemstra AM, Verfaillie SCJ, et al. Lower cerebral blood flow is associated with impairment in multiple cognitive domains in Alzheimer's disease. Alzheimers Dement. 2017;13:531–40.
17. Weijs RWJ, Shkredova DA, Brekelmans ACM, Thijssen DHJ, Claassen JAHR. Longitudinal changes in cerebral blood flow and their relation with cognitive decline in patients with dementia: current knowledge and future directions. Alzheimers Dement. 2023;19:532–48.
18. Nabizadeh F, Pourhamzeh M, Khani S, Rezaei A, Ranjbaran F, Deravi N, et al. Plasma phosphorylated-tau181 levels reflect white matter microstructural changes across Alzheimer's disease progression. Metab Brain Dis. 2022;37:761–71.
19. Nabizadeh F, Balabandian M, Rostami MR, Kankam SB, Ranjbaran F, Pourhamzeh M, et al. Plasma neurofilament light levels correlate with white matter damage prior to Alzheimer's disease: results from ADNI. Aging Clin Exp Res. 2022;34:2363–72.
20. Bettcher BM, Olson KE, Carlson NE, McConnell BV, Boyd T, Adame V, et al. Astrogliosis and episodic memory in late life: higher GFAP is related to worse memory and white matter microstructure in healthy aging and Alzheimer's disease. Neurobiol Aging. 2021;103:68–77.
21. Swinford CG, Risacher SL, Vosmeier A, Deardorff R, Chumin EJ, Dzemidzic M, et al. Amyloid and tau pathology are associated with cerebral blood flow in a mixed sample of nondemented older adults with and without vascular risk factors for Alzheimer's disease. Neurobiol Aging. 2023;130:103–13.
22. McDade E, Kim A, James J, Sheu LK, Kuan DC-H, Minhas D, et al. Cerebral perfusion alterations and cerebral amyloid in autosomal dominant Alzheimer disease. Neurology. 2014;83:710–7.
23. ElAli A, Thériault P, Préfontaine P, Rivest S. Mild chronic cerebral hypoperfusion induces neurovascular dysfunction, triggering peripheral beta-amyloid brain entry and aggregation. Acta Neuropathol Commun. 2013;1:75.

24. Koike MA, Green KN, Blurton-Jones M, LaFerla FM. Oligemic hypoperfusion differentially affects tau and amyloid-β. Am J Pathol. 2010;177:300–10.
25. Dubois B, Feldman HH, Jacova C, Hampel H, Molinuevo JL, Blennow K, et al. Advancing research diagnostic criteria for Alzheimer's disease: the IWG-2 criteria. Lancet Neurol. 2014;13:614–29.
26. Hughes CP, Berg L, Danziger W, Coben LA, Martin RL. A new clinical scale for the staging of dementia. Br J Psychiatry. 1982;140:566–72.
27. Folstein MF, Folstein SE, McHugh PR. Mini-mental state: a practical method for grading the cognitive state of patients for the clinician. J Psychiatr Res. 1975;12:189–98.
28. Dong H, Guo L, Yang H, Zhu W, Liu F, Xie Y, et al. Association between gray matter atrophy, cerebral hypoperfusion, and cognitive impairment in Alzheimer's disease. Front Aging Neurosci. 2023;15:10.
29. Smith SM, Jenkinson M, Johansen-Berg H, Rueckert D, Nichols TE, Mackay CE, et al. Tract-based spatial statistics: voxelwise analysis of multi-subject diffusion data. NeuroImage. 2006;31:1487–505.
30. Mori S, Oishi K, Jiang H, Jiang L, Li X, Akhter K, et al. Stereotaxic white matter atlas based on diffusion tensor imaging in an ICBM template. NeuroImage. 2008;40:570–82.
31. Hampel H, Hardy J, Blennow K, Chen C, Perry G, Kim SH, et al. The amyloid-β pathway in Alzheimer's disease. Mol Psychiatry. 2021;26:5481–503.
32. Karran E, Mercken M, Strooper BD. The amyloid cascade hypothesis for Alzheimer's disease: an appraisal for the development of therapeutics. Nat Rev Drug Discov. 2011;10:698–712.
33. Gao F, Dai L, Wang Q, Liu C, Deng K, Cheng Z, et al. Blood-based biomarkers for Alzheimer's disease a multicenter-based cross-sectional and longitudinal study in China. Sci Bull 2023;68:1800–8.
34. Ye BS, Seo SW, Kim GH, Noh Y, Cho H, Yoon CW. et al. Amyloid burden, cerebrovascular disease, brain atrophy, and cognition in cognitively impaired patients. Alzheimers Dement. 2015;11:494
35. Mattsson N, Tosun D, Insel PS, Simonson A, Jack CR, Beckett LA, et al. Association of brain amyloid-β with cerebral perfusion and structure in Alzheimer's disease and mild cognitive impairment. Brain. 2014;137:1550–61.
36. Maier FC, Wehrl HF, Schmid AM, Mannheim JG, Wiehr S, Lerdkrai C, et al. Longitudinal PET-MRI reveals β-amyloid deposition and rCBF dynamics and connects vascular amyloidosis to quantitative loss of perfusion. Nat Med. 2014;20:1485–92.
37. Park J-H, Hong J-H, Lee S-W, Ji HD, Jung J-A, Yoon K-W, et al. The effect of chronic cerebral hypoperfusion on the pathology of Alzheimer's disease: a positron emission tomography study in rats. Sci Rep. 2019;9:14102.
38. Janelidze S, Mattsson N, Palmqvist S, Smith R, Beach TG, Serrano GE, et al. Plasma P-tau181 in Alzheimer's disease: relationship to other biomarkers, differential diagnosis, neuropathology and longitudinal progression to Alzheimer's dementia. Nat Med. 2020;26:379–86.
39. Hansson O, Cullen N, Zetterberg H, Blennow K, Mattsson-Carlgren N.The Alzheimer's disease neuroimaging initiative Plasma phosphorylated tau181 and neurodegeneration in Alzheimer's disease. Ann Clin Transl Neurol. 2021;8:259–65.
40. Tissot C, Benedet AL, Therriault J, Pascoal TA, Lussier FZ, Saha-Chaudhuri P, et al. Plasma pTau181 predicts cortical brain atrophy in aging and Alzheimer's disease. Alzheimers Res Ther. 2021;13:11.
41. Moscoso A, Grothe MJ, Ashton NJ, Karikari TK, Lantero Rodríguez J, Snellman A, et al. Longitudinal associations of blood phosphorylated tau181 and neurofilament light chain with neurodegeneration in Alzheimer disease. JAMA Neurol. 2021;78:396.
42. Oeckl P, Halbgebauer S, Anderl-Straub S, Steinacker P, Huss AM, Neugebauer H, et al. Glial fibrillary acidic protein in serum is increased in Alzheimer's disease and correlates with cognitive impairment. J Alzheimers Dis. 2019;67:481–8.
43. Benedet AL, Milà-Alomà M, Vrillon A, Ashton NJ, Pascoal TA, Lussier F, et al. Differences between plasma and cerebrospinal fluid glial fibrillary acidic protein levels across the Alzheimer disease continuum. JAMA Neurol. 2021;78:1471.
44. Preman P, Alfonso-Triguero M, Alberdi E, Verkhratsky A, Arranz AM. Astrocytes in Alzheimer's disease: pathological significance and molecular pathways. Cells. 2021;10:540.
45. Pekny M, Pekna M, Messing A, Steinhäuser C, Lee J-M, Parpura V, et al. Astrocytes: a central element in neurological diseases. Acta Neuropathol. 2016;131:323–45.
46. Middeldorp J, Hol EM. GFAP in health and disease. Prog Neurobiol. 2011;93:421–43.
47. Shir D, Graff-Radford J, Hofrenning EI, Lesnick TG, Przybelski SA, Lowe VJ, et al. Association of plasma glial fibrillary acidic protein (GFAP) with neuroimaging of Alzheimer's disease and vascular pathology. Alzheimers Dement Diagn Assess Dis Monit. 2022;14:9.
48. Benedet AL, Leuzy A, Pascoal TA, Ashton NJ, Mathotaarachchi S, Savard M, et al. Stage-specific links between plasma neurofilament light and imaging biomarkers of Alzheimer's disease. Brain 2020;143:3793–804.
49. Illán-Gaia I, Lleo A, Karydas A, Staffaroni AM, Zetterberg H, Sivasankaran R, et al. Plasma tau and neurofilament light in frontotemporal lobar degeneration and Alzheimer disease. Neurology. 2021;96:E671–83.
50. Mielke MM, Syrjanen JA, Blennow K, Zetterberg H, Vemuri P, Skoog I, et al. Plasma and CSF neurofilament light Relation to longitudinal neuroimaging and cognitive measures. Neurology. 2019;93:E252–60.
51. Ten Kate M, Dicks E, Visser PJ, Van Der Flier WM, Teunissen CE, Barkhof F, et al. Atrophy subtypes in prodromal Alzheimer's disease are associated with cognitive decline. Brain. 2018;141:3443–56.
52. Deters KD, Shannon LRB, Kim S, Nhoa K, West JD, Blennow K, et al. Plasma tau association with brain atrophy in mild cognitive impairment and Alzheimer's disease. J Alzheimers Dis. 2017;58:1245–54.
53. Marks JD, Syrjanen JA, Graff-Radford J, Petersen RC, Machulda MM, Campbell MR, et al. Comparison of plasma neurofilament light and total tau as neurodegeneration markers: associations with cognitive and neuroimaging outcomes. Alzheimers Res Ther. 2021;13:14.
54. Sabuncu MR, Desikan RS, Sepulcre J, Yeo BTT, Liu HS, Schmansky NJ, et al. The dynamics of cortical and hippocampal atrophy in Alzheimer disease. Arch Neurol. 2011;68:1040–8.

ACKNOWLEDGEMENTS

This work was supported by Science and Technology Innovation 2030—Major Project (grant number 2021ZD0201805) and the Tianjin Key Medical Discipline (Specialty) Construction Project (grant number TJYXZDXK-004A).

AUTHOR CONTRIBUTIONS

YH and XJL processed and analyzed the imaging data. YH wrote the manuscript. FL, RXF, and YL collected clinical data and blood samples. PC was responsible for the plasma biomarker assay. WQ and YXZ conducted the MRI procedure and acquired the imaging data. NZ designed the study and revised the manuscript. The authors read and approved the final manuscript.

COMPETING INTERESTS

The authors declare no competing interests.

ETHICS APPROVAL AND CONSENT TO PARTICIPATE

The Ethics Committee of Tianjin Medical University General Hospital approved this study. Written informed consent was obtained from all participants. The present study was conducted in accordance with the Declaration of Helsinki.

ADDITIONAL INFORMATION

Correspondence and requests for materials should be addressed to Nan Zhang.